



Journal Name

## ARTICLE

This is a peer reviewed version of the following article: Phys. Chem. Chem. Phys. 2017, 19, 23254, which has been published in final form at <http://pubs.rsc.org/en/content/articlelanding/2017/cp/c7cp04295g#!divAbstract>.

## Guidelines and Diagnostics for Charge Carrier Tuning in Thiophene-Based Wires†

Ganna Gryn'ova, Pauline J. Ollitrault, Clémence Corminboeuf\*

Received 00th January 20xx,  
Accepted 00th January 20xx

DOI: 10.1039/x0xx00000x

[www.rsc.org/](http://www.rsc.org/)

Reported experimental trends in charge carrier tuning in single molecule junctions of oligothiophene-based wires are rationalized by means of frontier molecular orbital theory. The length and substituent effects on the frontier orbitals energy levels' are shown to translate to the computed transmission spectra – with a caveat of the role of the linker group. The resulting transport (charge carrier) type – *n*- (electrons) or *p*- (holes) – is easily identifiable from the *in silico* charge transfer trends.

### 1. Introduction

Single molecule junction (SMJ) architecture arises as an attractive and unique tactic for studying the intricate details of molecular charge, heat and force transport.<sup>1a</sup> SMJ experiments involving the scanning tunneling microscope break junction technique (STM-BJ)<sup>1b,c</sup> reveal the potential of a given system in such cutting-edge organic electronics applications as rectifiers, transistors, switches and logic circuits.<sup>1d-f</sup> Success of these systems depends, on one hand, upon an in-depth understanding of the chemical and physical factors governing their performance,<sup>1g</sup> and, on the other hand, necessitates the discovery of novel molecular motifs with targeted properties. Some of the most tantalizing research tasks include development of stable ambipolar and *n*-type materials, as well as systems with tunable transport channels.<sup>1h,i</sup>

In an SMJ, the transport type is generally defined by the frontier molecular orbital (MO) that is energetically the closest to the electrode material's Fermi level ( $E_F$ ): *p*-type (hole) transport in the case of the highest occupied molecular orbital (HOMO) and *n*-type (electron) transport in the case of the lowest unoccupied molecular orbital (LUMO, Fig. 1A).<sup>2</sup> At the orbital resonances the transmission,  $T(E)$ , is equal to 1, while within the HOMO-LUMO gap (HLG, also called the transport window) of the molecular wire the current is due to the

coherent off-resonant tunneling. When the Fermi level of an electrode falls into this gap, the conductance largely<sup>3</sup> corresponds to the tail of the transmission peak of the nearby MO.<sup>4</sup> Experimentally, the dominant charge carriers can be identified by the sign of the Seebeck coefficient (thermo-

Institut des Sciences et Ingénierie Chimiques, École polytechnique fédérale de Lausanne, CH-1015 Lausanne, Switzerland. E-mail: [clemence.corminboeuf@epfl.ch](mailto:clemence.corminboeuf@epfl.ch)  
† Electronic Supplementary Information (ESI) available: Full description of the computational procedures, complete set of results including the simulated transmission spectra and optimized geometries in the form of Gaussian archive entries. See DOI: 10.1039/x0xx00000x

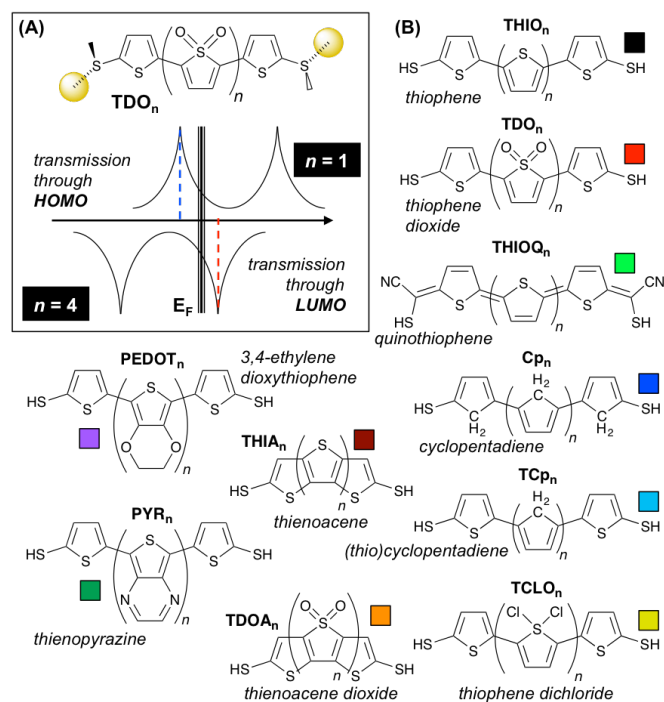


Fig. 1. (A) Schematic illustration of the energy level alignment between the molecule and the electrode that defines the nature of the charge carriers in oligothiophene S,S-dioxide wires of different lengths.<sup>8</sup> (B) Structures of the investigated wires with their custom abbreviations and color code, used throughout this work.

power): positive for the hole and negative for the electron transport.<sup>5</sup> External factors (such as electrochemical gating or highly polar environment)<sup>6</sup> aside, this energy level alignment between  $E_F$  and the molecular orbitals is thought to be strongly affected and even defined by the linker group: amine and thiol anchors form HOMO-conducting junctions, while pyridine and cyano groups lead to through-LUMO conductance.<sup>7</sup> However, in a recent study Campos, Venkataraman and co-workers elegantly demonstrated that the nature of the charge carriers could instead be tuned by molecular length (Fig. 1A).<sup>8</sup> Switching the transport type from  $p$ - to  $n$ - in  $\alpha$ -oligothiophene S,S-dioxide wires (TDO<sub>*n*</sub>), flanked by gold-binding (methylthio)thiophenes, was revealed by the change in the sign of Seebeck coefficient from positive (in TDO<sub>1</sub>) to negative (in TDO<sub>4</sub>). Compared to non-oxidized oligothiophene wires (THIO<sub>*n*</sub>), the measured conductance of the TDO<sub>*n*</sub> wires was higher and displayed a very shallow exponential decay<sup>9</sup> with molecular length. In contrast to TDO, an electron-donating substituent (–O– in 3,4-ethylenedioxythiophene, EDOT) was shown to destabilize the HOMO and promote the hole transport channel.<sup>10a</sup> Finally, rich transport behavior – *via* HOMO, mid-gap or LUMO – was achieved for electron-deficient  $\alpha$ -oligothiophene-based wires of similar lengths by varying the ring substitution.<sup>10b</sup>

These exciting discoveries attracted major attention in the SMJ community for developing tunable junctions. While molecular-level band-gap engineering techniques are fairly well understood in the field of conducting  $\pi$ -conjugated polymers,<sup>11–13</sup> they are not yet fully appreciated and exploited

in the single-molecule electronics arena. For example, the observed effect in the TDO<sub>*n*</sub> wires was rationalized as follows: *i*) upon oxidation, thiophene becomes antiaromatic and its LUMO is lowered by the electron-withdrawing oxo groups, *ii*) increase in the molecular length promotes planarization of the molecular backbone and leads to a stronger conjugation and LUMO delocalization.<sup>8,14</sup> These considerations, albeit intuitive, rely on not-so-well-defined concepts and rules-of-thumb,<sup>15</sup> exposing the need for a rigorous physical-chemical analysis of the charge carrier tunability. Moreover, this avenue of research still lacks a simple technique for forecasting the nature of charge carriers and the crossover point between the  $p$ - and  $n$ - transport types in a given wire.<sup>8</sup> In the present work, we scrutinize the molecular orbital and conductance trends in oligothiophene-derived wires of different lengths and substitution patterns using computational chemistry. Our findings lead to the design principles for SMJs with on-demand conductance characteristics and offer a simple *in silico* diagnostic of their transport types.

## 2. Computational Methods

In the present work, we employ density functional theory (DFT) and the non-equilibrium Green's function (NEGF) formalism<sup>16</sup> to investigate the orbital and length effects on the transport in the experimentally studied THIO<sub>*n*</sub> and TDO<sub>*n*</sub> wires<sup>8,10</sup>, as well as several other systems featuring various modifications to the thiophene ring and the terminal units of the chain (Fig. 1B,  $n = 1-4$  and selectively  $1-6^+$ ). For each system, we have assessed the electronic structure features of the individual molecules (at the  $\omega$ B97X-D/maug-cc-pVTZ//PBE0-D3/cc-pVDZ level of theory), as well as the geometric (PBE0-D3/cc-pVDZ with def2 ECP for Au atoms) and zero-bias transmission (PBE/DZP with ZORA) properties of their junctions with non-periodic Au(111) leads. These computations have been performed using the Gaussian 09, ADF 2016 and BAND 2016 software packages.<sup>17</sup> Detailed description and limitations of these methods are given in the ESI<sup>†</sup>.

## 3. Results and discussion

### 3.1 Substituent and chain lengths effects on molecular orbitals

Substituent effects on the frontier orbitals of the core thiophene ring can be rationalized using simple MO diagrams (Fig. 2A, provided the combining orbitals match by symmetry and energy)<sup>12,18</sup> and broadly split into several categories. Firstly, the electron-donating groups (EDGs) in the  $\beta$ -positions of the ring ( $\alpha$ -positions form the wire backbone) increase the substrate's HOMO level (consider the  $n=1$  datapoints for PEDOT and PYR cores relative to the dashed line for the reference THIO in Fig. 2C). The S-substituents do not affect the thiophene's HOMO since it has a nodal plane on the sulfur atom (Fig. 2B and D).<sup>5</sup> Secondly, the electron-withdrawing groups (EWGs) lower the substrate's LUMO (Fig. 2A). This is the case for all investigated S-substituted cores (TDO, TDOA,

TCLO, see Fig. 2C). Thirdly, additional combinations with other substituent MOs can have further impact: 1) the PEDOT's LUMO is higher than the THIO's (due to the combination of the EDG's HOMO-1 with the thiophene's LUMO), 2) the PYR's LUMO is lower than THIO's (it combines with the thiophene's LUMO), 3) the TDO's, TCLO's and TDOA's HOMOs are all lower than the THIO's (combination of the EWG's  $n^*$  unoccupied MO with the thiophene's HOMO, see the shaded diagrams in Fig. 2A and Fig. S2A, B in the ESI<sup>†</sup>). Frontier molecular orbital plots for the representative systems are shown in Fig. 2D, while Fig. S9 in the ESI<sup>†</sup> contains these plots for all investigated wires. Finally, alterations to the thiophene rings and their interconnectivity also influence the frontier orbitals: the fused analogues of THIO and TDO – THIA and TDOA – have somewhat larger HLGs,<sup>18,19</sup> while the cyclopentadiene (Cp) HOMO is less stabilized than the HOMO of the aromatic THIO. In a quinoidal THIOQ core, the HOMO and the LUMO are swapped compared to THIO leading to a significantly lower HLG and making quinothienophenes efficient  $n$ -channel organic field-effect transistors.<sup>20</sup> Importantly, since the  $n=1$  systems feature one variable core between the two (2-thio)thiophene rings, their orbitals (particularly the HOMO) are strongly affected by these terminal linker groups (compare Cp<sub>1</sub> and TCp<sub>1</sub> in Fig. 2C). In addition to these substituent effects, the chain growth (larger  $n$ ) further affects the MO energy trends. As in the classical polyene series, increasing conjugation length is associated with the shrinking HLG (mirrored by the experimentally measured optical gaps).<sup>11,21</sup> This is the case for all studied wires with  $n$  going from 1 to 4 (Fig. 2C and Fig. S2C in the ESI<sup>†</sup>). While in THIO <sub>$n$</sub>  both frontier orbital levels 'move', in the extreme case of PEDOT <sub>$n$</sub> , only the HOMO energy is changing continuously. The energy level splitting between the neighbor cores does formally lower its LUMO energy, but the effect is counteracted by the aforementioned LUMO heightening in each individual core, thus the resulting LUMO level is largely unchanged despite the increasing  $n$ . The HOMO levels in the TCLO <sub>$n$</sub> , TDOA <sub>$n$</sub>  and TDO <sub>$n$</sub>  series are subject to

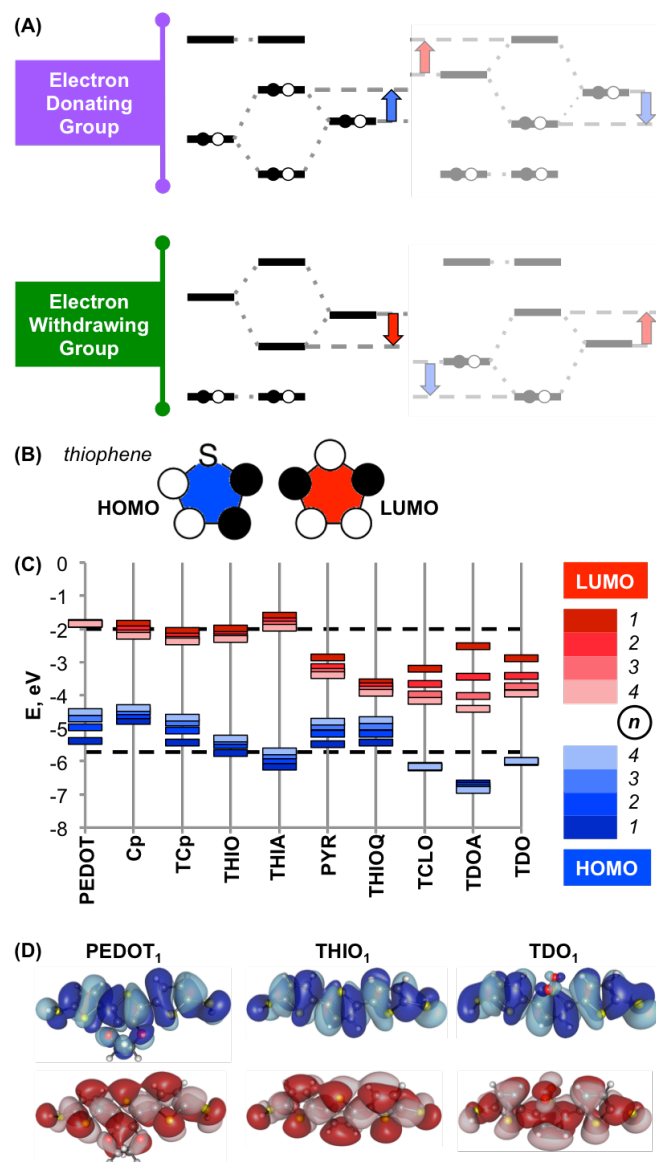


Fig. 2. (A) Schematic MO diagrams illustrating the substituent effects on the frontier orbital energy levels. (B) Schematic HOMO and LUMO plots of a non-substituted thiophene ring. (C) Computed (PBE0/cc-pVDZ) frontier orbital energy levels for  $n=1-4$  wires (the dashed horizontal lines denote the 'reference' orbital levels of THIO<sub>1</sub>). (D) HOMO (blue) and LUMO (red) plots (PBE0/cc-pVDZ level of theory, isovalue = 0.020) for representative systems with  $n=1$ , see the ESI<sup>†</sup> for the HOMO and LUMO plots of all studied wires with  $n=1-6$ .

similar effects. All these trends, reproduced in the ionization potentials and electron affinities (Fig. S3, ESI<sup>†</sup>), clearly demonstrate that a diverse array of the oligothiophenes' frontier orbitals can be accessed *via* simple modifications and substitutions to the thiophene cores and the architectures of their wires.

### 3.2 The role of orbitals in the transmission spectra of the wires

Once the guidelines for manipulating the wire's MO energies are established, the question arises of whether they persist in the SMJs and translate into the dominant conductance channels. We find that the peak positions in the computed transmission spectra largely follow the orbital energy levels in

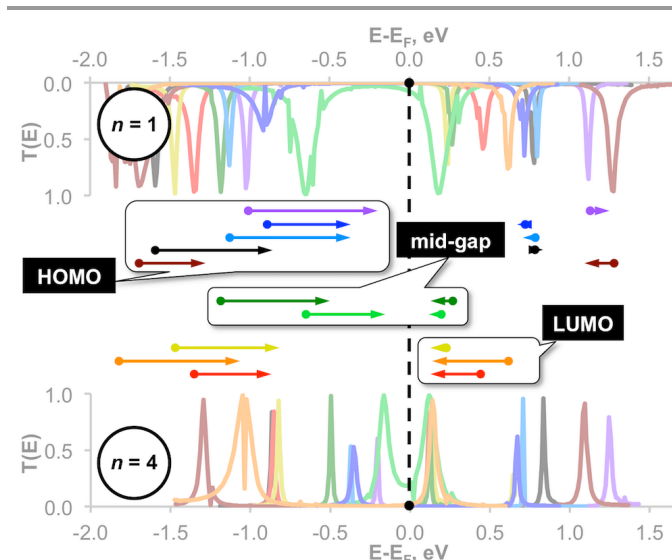


Fig. 3. Computed transmission spectra (only the peaks corresponding to the HOMO and LUMO resonances are shown for clarity) of all studied wires (see the color code in Fig. 1B) for  $n=1$  (top) and  $n=4$  (bottom). The middle panel shows the shifts of the transmission peaks and indicates the likely transport channel.

the isolated molecules (Fig. S4, ESI<sup>†</sup>). However, the conductance peaks due to HOMO move closer to the  $E_F$  with increasing  $n$  in all systems, including  $TDO_n$ ,  $TDOA_n$  and  $TCLO_n$  in which the HOMO energy level is fairly constant (Fig. 2C). This is due to the HOMO-conducting linker, (2-thio)thiophene, which affords substantial coupling between the HOMO and the lead's valence band. The positions of the transmission peaks corresponding to the frontier MOs relative to the computed  $E_F$  are subject to the ambiguity in the level alignment, discussed at length in the ESI<sup>†</sup>. Importantly, the transmission peaks progressively shift towards the  $E_F$  with increasing  $n$  and these shifts correlate well with the experimentally detected transport types (Fig. 3).<sup>8,22</sup> The  $PEDOT_n$ ,  $THIO_n$ ,  $THIA_n$ ,  $Cp_n$  and  $TCp_n$  wires display significant shifts of the HOMO (but not the LUMO) resonances suggesting the through-HOMO transport type. On the other hand, in the  $TDO_n$ ,  $TDOA_n$  and  $TCLO_n$  wires, the peaks due to LUMO shift very close towards the Fermi level, indicative of the  $n$ -channel conductance. Finally, in  $PYR_n$  and  $THIOQ_n$  the peaks of both the HOMO and the LUMO resonances approach  $E_F$  as  $n$  increases, suggesting mid-gap transport *via* their superimposed tails.<sup>11</sup>

### 3.3 Charge transfer as a transport type diagnostic

In addition to the transmission peak positions and the signs of the Seebeck coefficients, charge transfer between the molecule and the leads reflects the nature of the transport: through-LUMO conductance involves an initial electron injection from the lead to the molecule, while the HOMO transport entails an opposite process.<sup>23</sup> Thus, the  $n$ -type transport is associated with the positive leads and a negative molecule ( $\Delta Q < 0$  with respect to the latter),  $p$ -transport – positive molecule and negative leads ( $\Delta Q > 0$ ). Fig. 4A shows the trends in the charge transfer (based on Hirshfeld population analysis) depending on  $n$  in the studied junctions, which can be accordingly split into three categories: 1) increasing  $n$

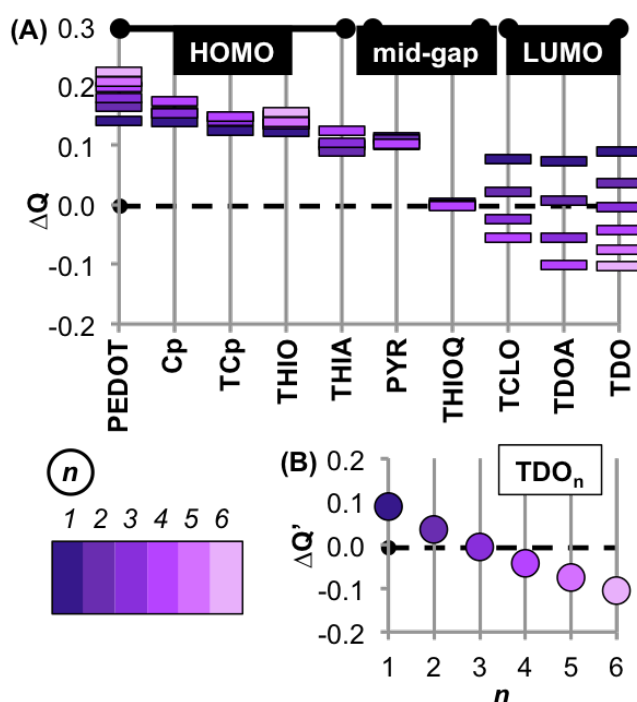


Fig. 4. (A) Charge transfer from the molecule to the leads ( $\Delta Q > 0$ ) based on the PBE/DZP+ZORA Hirshfeld population analysis in all studied systems with  $n=1-4$  (and selectively 1-6) (A) and in  $TDO_n$  junctions (B).

promotes the electron donation from the molecule to the leads, consistent with through-HOMO transport; 2) increasing  $n$  promotes the electron injection from the leads to the molecule, consistent with through-LUMO transport; 3) charge transfer independent on  $n$ , suggesting the mid-gap transport. The charge transfer trends in the  $TDO_n$  wires (Fig. 4B) are in a very good agreement with the dominant transport channels, proposed on the basis of the measured Seebeck coefficients: through-HOMO in  $TDO_1$ , through both orbitals in  $TDO_2$  and  $TDO_3$  and through-LUMO in  $TDO_4$ .<sup>8</sup>

### 3.4 The length decay of the wires' conductances

We have also assessed the length-dependence of the computed conductance.<sup>9</sup> The conductance decay constant,  $\beta$ , is estimated from  $G \approx \exp(-\beta L)$ , where  $L$  is the transport length (taken in this work as the distance between the sulfur atoms of the  $-SH$  linkers). To estimate  $\beta$  in the off-resonant tunneling regime (Fig. S6, ESI<sup>†</sup>) we use the conductance values in the middle of the transport gap.<sup>24</sup> Resulting decay constants (Fig. 5A) agree reasonably well with the literature:  $0.2 \text{ \AA}^{-1}$  in  $TDO_n$  wires<sup>8</sup> and a range of values for the non-oxidized oligothiophene-based wires –  $0.30-0.71 \text{ \AA}^{-1}$ ,<sup>22</sup>  $0.32 \text{ \AA}^{-1}$ ,<sup>25a</sup>  $0.296 \text{ \AA}^{-1}$ ,<sup>25b</sup>  $0.19 \text{ \AA}^{-1}$ ,<sup>25c</sup>  $0.211 \text{ \AA}^{-1}$ .<sup>23</sup> Our computed mid-gap  $G/G_0$  values deviate from the exponential decay<sup>22,26</sup> and follow an oscillating trend (being higher for even  $n$  than for odd)<sup>26c,d</sup> due to non-equality of the terminal binding geometries for odd  $n$  wires (Fig. S7, ESI<sup>†</sup>). However, this trend is a result of a static approach to the model junction geometries and is suppressed in the experimental setup, where conductance values are measured over thousands of counts. Instead, the planarity of

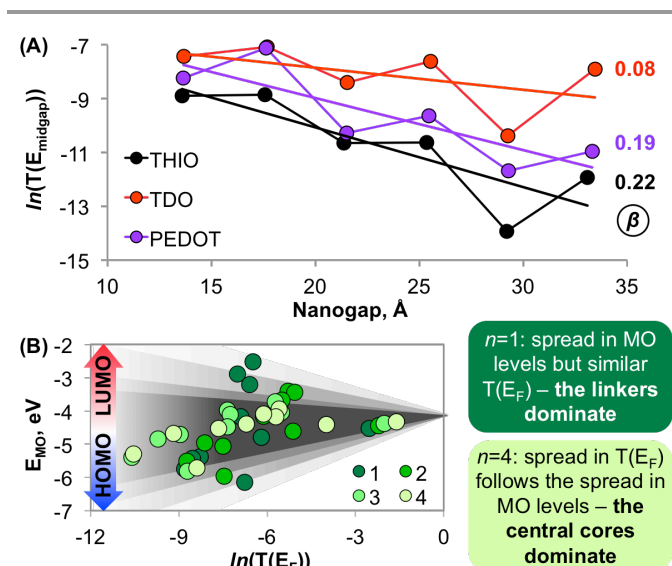


Fig. 5. (A) Computed transmissions (in  $G/G_0$  units) in the middle of the transport gap for selected wires with  $n = 1-6$  (numbers in color are the estimated decay constants). (B) PBE0/cc-pVDZ+ECP energy levels of the molecular orbitals dominating the conductance (HOMO for THIO<sub>n</sub>, THIA<sub>n</sub>, PEDOT<sub>n</sub>, Cp<sub>n</sub> and TCp<sub>n</sub>, LUMO for TDO<sub>n</sub>, TDOA<sub>n</sub> and TCLO<sub>n</sub>, mid-HLG for PYR<sub>n</sub> and THIOQ<sub>n</sub>) plotted against the computed PBE/DZP+ZORA  $T(E_F)$  for all studied systems with  $n = 1-4$ .

the wires is known to impact upon their experimentally measured conductance<sup>27</sup> since it directly affects the extent of conjugation and the associated orbital level splitting. Indeed, the optimized junction geometries for THIO<sub>n</sub> wires show larger deviations from 180° than TDO<sub>n</sub> and PEDOT<sub>n</sub> (Fig. S8, ESI<sup>†</sup>) and, for a given  $n$ , computed conductance of a THIO<sub>n</sub> wire is lower than that of TDO<sub>n</sub> and PEDOT<sub>n</sub>, in line with the measured trends.<sup>8</sup>

Provided the influences on the level alignment that arise on the junction level, the question remains of whether the molecular-level factors (*e.g.*, the substituent effects) still govern the charge transport in the SMJs. As illustrated in Fig. 5C, the closer the energy of the orbital (in an isolated molecule) dominating the transport to a certain energetic threshold (corresponding to  $E_F$  in the junction), the higher the apparent conductance.<sup>¶</sup> This tendency becomes more pronounced with increasing  $n$  as the influence of the electronic structure of the individual building units surpasses that of the (2-thio)thiophene linkers.

## Conclusions

In summary, we have rationalized the factors that govern the frontier orbitals' energy levels in various oligothiophene-based wires. These orbital energies depend on the electronic effects (*e.g.*, the substituents) in the central cores, their interconnectivity (such as the quinodal structure) and number (wire length). Most importantly, they directly translate to the conductance peaks positions and, together with the linker group, define the zero-bias transmission. Furthermore, the charge transfer trends in the optimized junctions, easily accessed through inexpensive computations, qualitatively reflect the molecular length-driven crossover between  $n$ - and

$p$ - transport types. These findings provide a conceptual framework to the stimulating recent experimental work<sup>8,10</sup> and offer orbital guidelines and *in silico* diagnostics for the molecular design of single molecule junctions with targeted charge transport characteristics.

## Acknowledgements

This work has received funding from the European Union's Horizon 2020 research and innovation programme under the Marie Skłodowska-Curie grant agreement No. 701885 and financial and infrastructural support from EPFL. The authors thank Mr Alberto Fabrizio and Dr Jian-Hao Li for helpful discussions.

## Notes and references

‡ At large molecular lengths (above  $\sim 25\text{Å}$ ) the transport mechanism changes from coherent off-resonant tunneling to sequential thermally activated hopping,<sup>28</sup> however the latter has not been included in this study and our results for wires with  $n > 4$  are meaningful only to obtain the projected trends in the coherent tunneling regime.

§ For this simple interpretation, we neglect the secondary orbital effects, such as hyperconjugation between the thiophene and S-substituent.

¶ Experimentally reported<sup>20</sup> quinoidal oligothiophenes are flanked with the EWGs and are classified as  $n$ -type materials. In this study, the end groups carry both an electron donor with through-HOMO conductance ( $-\text{SH}$ ) and an electron acceptor with through-LUMO conductance ( $-\text{CN}$ )<sup>7b</sup> and are therefore likely to involve mixed (mid-gap) transport.

¶ The scatter in this graph is largely due to non-equal nanogaps for a given  $n$  between different cores (Table S1, ESI<sup>†</sup>) and the odd/even effects due to the static geometry treatment.

- (a) L. Sun, Y. A. Diaz-Fernandez, T. A. Gschneidner, F. Westerlund, S. Lara-Avila and K. Moth-Poulsen, *Chem. Soc. Rev.*, 2014, **43**, 7378; (b) B. Q. Xu and N. J. Tao, *Science*, 2003, **301**, 1221; (c) E. Scheer, N. Agrait, J. C. Cuevas, A. L. Yeyati, B. Ludophk, A. Martín-Rodero, G. R. Bollinger, J. M. van Ruitenbeek and C. Urbina, *Nature*, 1998, **394**, 154; (d) D. Xiang, X. Wang, C. Jia, T. Lee and X. Guo, *Chem. Rev.*, 2016, **116**, 4318; (e) J. Del Nero, F. M. de Souza and R. B. Capaz, *J. Comput. Theor. Nanosci.*, 2010, **7**, 1; (f) H. Song, M. A. Reed and T. Lee, *Adv. Mater.*, 2011, **23**, 1583; (g) T. A. Su, M. Neupane, M. L. Steigerwald, L. Venkataraman and C. Nuckolls, *Nat. Reviews*, 2016, **1**, 16002; (h) Y. Zhao, Y. Guo and Y. Liu, *Adv. Mater.*, 2013, **25**, 5372; (i) J. E. Anthony, A. Facchetti, M. Heeney, S. R. Marder and X. Zhan, *Adv. Mater.*, 2010, **22**, 3876.
- (a) Y. Tsuji and R. Hoffmann, *Angew. Chem. Int. Ed.*, 2014, **53**, 4093; (b) J. R. Quinn, F. W. Foss Jr., L. Venkataraman and R. Breslow, *J. Am. Chem. Soc.*, 2007, **129**, 12376.
- In the off-resonant transport, both  $\pi$ - and  $\sigma$ -systems contribute significantly to the overall conductance, see G. C. Solomon, D. Q. Andrews, R. P. Van Duyne and M. A. Ratner, *ChemPhysChem*, 2009, **10**, 257.
- C. Joachim and J. F. Vinuesa, *Europhys. Lett.*, 1996, **33**, 635.

- 5 K. Baheti, J. A. Malen, P. Doak, P. Reddy, S.-Y. Jang, T. D. Tilley, A. Majumdar and R. A. Segalman, *Nano Lett.*, 2008, **8**, 715.
- 6 (a) C. Huang, A. V. Rudnev, W. Hong and T. Wandlowski, *Chem. Soc. Rev.*, 2015, **44**, 889; (b) B. Capozzi, J. Xia, O. Adak, E. J. Dell, Z.-F. Liu, J. C. Taylor, J. B. Neaton, L. M. Campos and L. Venkataraman, *Nat. Nanotechnol.*, 2015, **10**, 522.
- 7 (a) J. R. Widawsky, P. Darancet, J. B. Neaton and L. Venkataraman, *Nano Lett.*, 2012, **12**, 354; (b) L. A. Zotti, T. Kirchner, J.-C. Cuevas, F. Pauly, T. Huhn, E. Scheer and A. Erbe, *small*, 2010, **6**, 1529; (c) V. Obersteiner, D. A. Egger and E. Zojer, *J. Phys. Chem. C*, 2015, **119**, 21198.
- 8 E. J. Dell, B. Capozzi, J. Xia, L. Venkataraman and L. M. Campos, *Nature Chem.*, 2015, **7**, 209.
- 9 K. H. Khoo, Y. Chen, S. Li and S. Y. Quek, *Phys. Chem. Chem. Phys.*, 2015, **17**, 77.
- 10 (a) B. Capozzi, J. Z. Low, J. Xia, Z.-F. Liu, J. B. Neaton, L. M. Campos and L. Venkataraman, *Nano Lett.*, 2016, **16**, 3949; (b) J. Z. Low, B. Capozzi, J. Cui, S. Wei, L. Venkataraman and L. M. Campos, *Chem. Sci.*, 2017, **8**, 3254.
- 11 S. S. Zade and M. Bendikov, *Org. Lett.*, 2006, **8**, 5243.
- 12 A. L. Botelho, Y. Shin, J. Liu and X. Lin, *PLoS ONE*, 2014, **9**, e86370.
- 13 (a) H. A. M. van Mullekom, J. A. J. M. Vekemans and E. W. Meijer, *Chem. Eur. J.*, 1998, **4**, 1235; (b) A. K. Bakhshi, A. Kaur and V. Arora, *Ind. J. Chem.*, 2012, **51A**, 57; (c) Y.-C. Hung, C.-Y. Chao, C.-A. Dai, W.-F. Su and S.-T. Lin, *J. Phys. Chem. B*, 2013, **117**, 690.
- 14 A. Pramanik and P. Sarkar, *Phys. Chem. Chem. Phys.*, 2015, **17**, 26703.
- 15 J. F. Gonthier, S. N. Steinmann, M. D. Wodrich and C. Corminboeuf, *Chem. Soc. Rev.*, 2012, **41**, 4671.
- 16 (a) J. Maassen, M. Harb, V. Michaud-Rioux, Y. Zhu and H. Guo, *Proc. IEEE*, 2013, **101**, 518; (b) S. Y. Quek and K. H. Khoo, *Acc. Chem. Res.*, 2014, **47**, 3250; (c) J. S. Seldenthuis, PhD thesis, TU Delft, 2011; (d) C. J. O. Verzijl and J. M. Thijssen, *J. Phys. Chem. C*, 2012, **116**, 24393.
- 17 (a) M. J. Frisch *et al.* **Gaussian 09**, Revision **D.01**, Gaussian, Inc.: Wallingford CT, 2009. For the full reference, see Ref. 1 in the ESI<sup>†</sup>; (b) G. te Velde, F. M. Bickelhaupt, E. J. Baerends, C. Fonseca Guerra, S. J. A. van Gisbergen, J. G. Snijders and T. Ziegler, *J. Comput. Chem.*, 2001, **22**, 931; (c) C. Fonseca Guerra, J. G. Snijders, G. te Velde and E. J. Baerends, *Theor. Chem. Acc.*, 1998, **99**, 391; (d) **ADF2016** and **BAND2016**, SCM, Theoretical Chemistry, Vrije Universiteit, Amsterdam, The Netherlands, <http://www.scm.com>.
- 18 M. Wykes, B. Milián-Medina and J. Gierschner, *Front. Chem.*, 2013, **1**, 35.
- 19 X. Zhang, A. P. Côté and A. J. Matzger, *J. Am. Chem. Soc.*, 2005, **127**, 10502. Note this comparison is indirect since THIO<sub>1</sub> has altogether six C=C bonds, while THIA<sub>1</sub> – only four.
- 20 Y. Suzuki, M. Shimawaki, E. Miyazaki, I. Osaka, K. Takimiya, *Chem. Mater.*, 2011, **23**, 795.
- 21 (a) D. Ghosh, J. Hachmann, T. Yanai and G. K.-L. Chan, *J. Chem. Phys.*, 2008, **128**, 144117; (b) J. L. Brédas, R. Silbey, D. S. Boudreaux and R. R. Chance, *J. Am. Chem. Soc.*, 1983, **105**, 6555; (c) The various energy gaps should be discussed with care, see J.-L. Brédas, *Mater. Horiz.*, 2014, **1**, 17.
- 22 (a) E. J. Dell, PhD thesis, Columbia University, 2015; (b) P. Li, Y. Cui, C. Song and H. Zhang, *J. Phys. Chem. C*, 2016, **120**, 14484 (note that the modeling is on the single crystals rather than the SMJs).
- 23 G. Peng, M. Strange, K. S. Thygesen and M. Mavrikakis, *J. Phys. Chem. C*, 2009, **113**, 20967.
- 24 (a) C. Brooke, A. Vezzoli, S. J. Higgins, L. A. Zotti, J. J. Palacios and R. J. Nichols, *Phys. Rev. B*, 2015, **91**, 195438; (b) D. Nozaki, Y. Girard and K. Yoshizawa, *J. Phys. Chem. C*, 2008, **112**, 17408.
- 25 (a) L. Xiang, T. Hines, J. L. Palma, X. Lu, V. Mujica, M. A. Ratner, G. Zhou and N. Tao, *J. Am. Chem. Soc.*, 2016, **138**, 679; (b) W. B. Chang, C.-K. Mai, M. Kotiuga, J. B. Neaton, G. C. Bazan and R. A. Segalman, *Chem. Mater.*, 2014, **26**, 7229; (c) Y. Ie, M. Endou, A. Han, R. Yamada, H. Tada and Y. Aso, *Pure Appl. Chem.*, 2012, **84**, 931.
- 26 (a) B. Q. Xu, X. L. Li, X. Y. Xiao, H. Sakaguchi and N. J. Tao, *Nano Lett.*, 2005, **5**, 1491; (b) J. Zhang, W. Sun, H. Liu, Y. He and J. Zhao, *Comput. Mater. Sci.*, 2014, **87**, 100; (c) V. K. Lamba, S. Engles, P. Yadav and S. Dhanda, *Proc. SPIE*, 2012, **8549**, 85492Z-1; (d) L. Jiang, C. S. S. Sangeeth and C. A. Nijhuis, *J. Am. Chem. Soc.*, 2015, **137**, 10659.
- 27 (a) L. Venkataraman, J. E. Klare, C. Nuckolls, M. S. Hybertsen and M. L. Steigerwald, *Nature*, 2006, **442**, 904; (b) E. J. Dell, B. Capozzi, K. H. Dubay, T. C. Berkelbach, J. R. Moreno, D. R. Reichman, L. Venkataraman and L. M. Campos, *J. Am. Chem. Soc.*, 2013, **135**, 11724.
- 28 (a) T. Hines, I. Diez-Perez, J. Hihath, H. Liu, Z.-S. Wang, J. Zhao, G. Zhou, K. Müllen and N. Tao, *J. Am. Chem. Soc.*, 2010, **132**, 11658; (b) C. E. Smith, S. O. Odoh, S. Ghosh, L. Gagliardi, C. J. Cramer and C. D. Frisbie, *J. Am. Chem. Soc.*, 2015, **137**, 15732.